Constructing Human Atrial Electrophysiological Models Mimicking a Patient-Specific Cell Group

A Muszkiewicz[1,2], A Bueno-Orovio[1], X Liu[3], B Casadei[3], B Rodriguez[1]

[1] Department of Computer Science, University of Oxford, Oxford, UK
[2] Systems Biology Doctoral Training Centre, University of Oxford, Oxford, UK
[3] Division of Cardiovascular Medicine, University of Oxford, Oxford, UK

Abstract

Patient-specific modelling aims to produce computational models of human physiology tailored to a specific patient. In line with this, we construct multiple human atrial electrophysiological models mimicking the behaviour of single atrial myocytes extracted from a homogeneous patient group. We study cells with the action potential duration being 2–3 times lower than in human atrial electrophysiological models. Assuming such a difference can be rationalized by altering the values of ionic conductances, we generated 15000 models by simultaneously varying conductance values of the most important currents affecting the action potential (AP). We paced the models at different frequencies and conditions, probing the importance of ion concentrations and stimulus strength, and kept the models producing AP biomarkers consistent with experiments. We discovered that both the ionic conductances and external factors play a critical role in producing biomarker values consistent with experiments. By mimicking experimental conditions, we generated 604 models fully covering the experimental range of AP biomarkers. In conclusion, both the ionic conductances and external factors are vital in tailoring single-cell electrophysiological models to a narrow patient group. This has implications in understanding the propensity of subgroups of the total population to disease conditions.

1. Introduction

Models of human atrial electrophysiology described in the literature are constructed with experimental data obtained from different cells studied with a variety of techniques. They are also based on information averaged over multiple cells, and produce a single action potential trace designed to represent the 'typical' behaviour of atrial myocytes. Therefore, these models are likely to produce results that are (a) not representative of any atrial myocyte in particular, and therefore (b) unlikely to reflect properties of cells extracted from different groups of patients.

Using experimental single-cell data, we aimed to construct multiple models of human atrial electrophysiology mimicking the behaviour seen in a narrow patient group. For this purpose, we used the action potential (AP) data measured in 18 atrial myocytes extracted from 8 elderly male patients in sinus rhythm and undergoing coronary artery bypass graft in Oxford, UK. This dataset is challenging to model because some of the AP biomarkers recorded in experiments are 2–3 times smaller than in the biophysically-detailed models of human atrial electrophysiology. Specifically, the experimental values of the action potential duration at 90% repolarization (APD_{90}) are in the range $80 - 150$ ms, compared to the typical model values of $300 - 350$ ms [1]. Furthermore, the resting membrane potential measured in these cells spans 15 mV with a maximum of -70 mV, compared to a single value of -75 mV produced by the models. This highlights the importance of constructing multiple electrophysiological models in order to capture a large range of values that a specific biomarker can take. Therefore, we decided to construct a population of models calibrated with experimental AP data [2].

2. Methods

2.1. Experimental biomarkers

The five biomarkers used in this study are resting membrane potential (RMP), action potential amplitude (APA), and action potential duration at 20%, 50%, and 90% repolarization (APD_{20}, APD_{50}, APD_{90}). These were measured for every cell at five stimulation frequencies: 0.25, 0.5, 1, 2, and 3Hz [3]. Table 1 shows minimum and maximum values of the biomarkers at two selected frequencies.

2.2. Population of single-cell models

APs generated in the experiments displayed a triangular morphology, reminiscent of that seen in the Maleckar *et*

Table 1. Ranges of the AP biomarker values used in the calibration process for two selected frequencies.

Biomarker	1Hz	3Hz
RMP (mV)	[-85.2, -69.4]	[-87.2, -68.1]
APA (mV)	[94.6, 127.1]	[97.9, 128.4]
APD_{20} (ms)	[2.7, 11.5]	[3.1, 11.6]
APD_{50} (ms)	[9.4, 34.1]	[10.0, 37.1]
APD_{90} (ms)	[63.4, 142.8]	[64.8, 131.6]

al. model of human atrial electrophysiology [4]. Therefore, we based our population of single-cell models on this framework. Since the ionic current conductances are known to display significant intercellular variability, we assumed that altering their values would be sufficient to reproduce the AP characteristics observed in this patient group. The 11 conductances altered in this study corresponded to the membrane currents I_{Kur}, I_{Kr}, I_{Ks}, I_{to}, I_{K1}, $I_{Ca,L}$, I_{Na}, the currents regulating calcium influx and efflux in the sarcoplasmic reticulum J_{up} and J_{rel}, as well as membrane pumps and exchangers I_{NaK} and I_{NCX}. All 11 conductances were varied simultaneously within $\pm 100\%$ range from their baseline model values with Latin Hypercube sampling, which generates parameter sets over a large number of parameters efficiently and without bias [2]. Overall, an initial population consisting of 15000 models was generated in this manner.

2.3. Simulation protocol

Every model within the population was simulated in conditions resembling experiments as closely as possible. That is, the cytosolic and extracellular ionic concentrations were adjusted to the values used in experiments. Each model was stimulated for 100 beats at every frequency. The impact of ionic concentrations on the AP biomarkers produced by the models was assessed in a series of simulations, where (a) all ionic concentrations in the models were allowed to vary, (b) cytosolic and effective extracellular potassium concentrations were held constant, and (c) cytosolic potassium and sodium, as well as effective extracellular potassium, sodium and calcium were fixed. Likewise, the influence of the stimulus strength on the biomarkers was assessed by scaling its baseline model value by factors ranging from 1.0 to 0.5 in 0.1 steps.

The simulations were performed using CHASTE, the open source software framework designed for modelling in computational biology [5]. Numerical integration was performed with CVODE, an ordinary differential equation solver with a varying time step, with absolute and relative error tolerances set to 10^{-9} and 10^{-10}, respectively. Biomarkers were calculated every 1 ms.

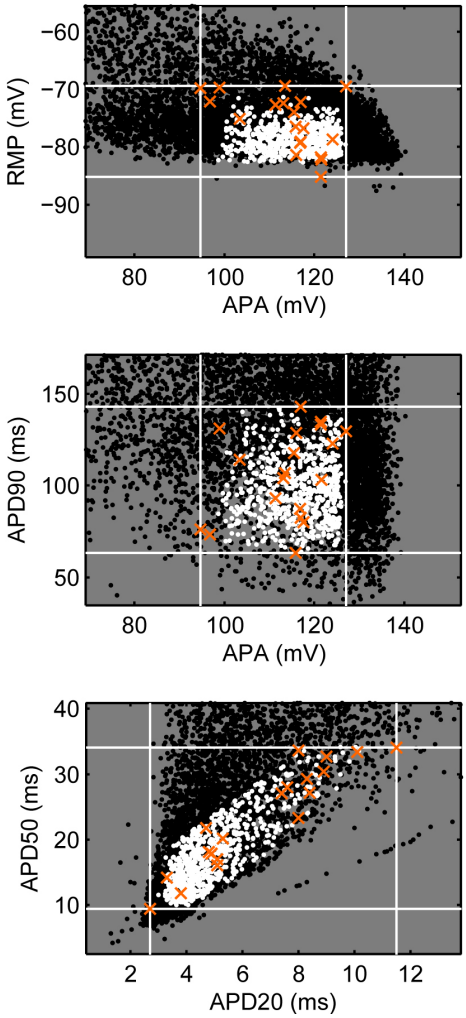

Figure 1. Selected biomarker plots illustrating the coverage of the biomarker space at 1Hz. Legend: orange crosses – experimental datapoints; white dots – accepted models; black dots – rejected models; white lines – limits of the experimentally allowed biomarker values. Accepted models cover the experimentally available biomarker space well, albeit the higher values of APD_{20} and APD_{50} are sampled less densely than the rest of the space.

2.4. Calibration

Following the simulations, the initial population of models was calibrated against the experimental data. That is, we checked whether the biomarker values generated by a specific model at every stimulation frequency fell within the ranges observed in experiments; the experimentally allowed range was defined by the minimum and maximum values of the specific biomarker at a particular frequency. If all these criteria were met, the model was accepted for further investigations.

3. Results

3.1. Coverage of the biomarker space

The first series of simulations (with all ionic concentrations free to vary), resulted in 164 accepted models with a good coverage of APD_{90} and APA biomarkers. However, the models also displayed an increase in RMP with pacing frequency not observed in experiments. This was especially restrictive at the highest frequency of 3Hz, where the accepted models displayed RMP ranging between -71 mV and -68 mV, which corresponded to the uppermost end of the experimental range covering -87 mV to -68 mV. Furthermore, the APD_{20} biomarkers produced by the accepted models were located in the lower third of their experimental ranges. The initial poor coverage of several AP biomarkers motivated further investigations to refine the populations of models.

RMP of excitable cells is predominantly determined by the reversal potential of potassium ions, which is in turn related to the ratio of the extracellular to cytosolic potassium concentration. The model of Maleckar *et al.* contains the cleft space surrounding the cytosol, acting as an effective extracellular space. Crucially, local accumulation or depletion of ions relative to the bulk is permitted in the cleft space. At high pacing frequencies, potassium ions accumulate in this space, thereby increasing the RMP. We addressed this problem by clamping both the cytosolic and the effective extracellular potassium concentrations to a constant value matching the relevant experimental concentrations. While this partly alleviated the problem, the RMP was still increasing at high pacing frequencies, albeit more slowly. Following Cherry *et al.* [6], we decided to additionally clamp the cytosolic and cleft concentrations of sodium and the cleft concentration of calcium to their experimental values. The resultant 282 accepted models spanned the experimentally permitted range of RMP values at all frequencies.

APD20 is highly influenced by the stimulus strength applied to the models: a larger magnitude of the stimulus will produce a larger APA and a smaller APD_{20}. Since all accepted models had short APD_{20} values, we decreased the stimulus strength in increments of 10% starting from the baseline model value. Reducing the stimulus strength to $1/2$ of its original value increased the number of accepted models to 604 and produced a good coverage of the biomarker space for all biomarkers (Figure 1).

3.2. Conductances in accepted models

The majority of the conductances underpinning the 604 accepted models are spread within $\pm 35\%$ of the median (Figure 2), indicating that most of the unusual parameter values were rejected in the calibration process. Medians of

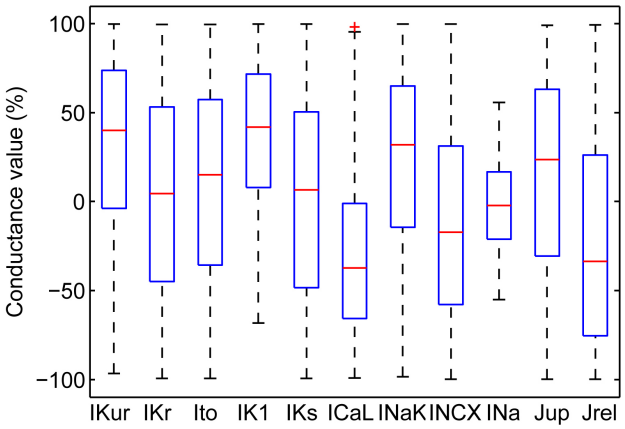

Figure 2. Box plot of the ionic current conductances in the accepted models. The majority of the conductance values underpinning the 604 accepted models are spread within $\pm 35\%$ of the median, indicating that most of the unusual parameter values were rejected in the calibration process.

8 out of 11 varied parameters differ by more than $\pm 10\%$ relative to the baseline model values. This is to be expected in view of the significant differences between the biomarkers produced by the baseline model and the cells in experiments.

Investigations into the links between specific parameter values and AP biomarkers revealed that the models producing APD values at the higher end of the experimentally allowed range display a significant reduction in the conductance of the transient outward potassium current, G_{to}. In these models, G_{to} ranges between -100% and -40% of the baseline model value, corresponding to the bottom whisker on the box plot in Figure 2. Therefore, in order to further improve the biomarker space sampling in the region of higher APD values, one could generate two populations of models: one with G_{to} distributed within $\pm 40\%$ of the median, and another one with the parameter scaled down in the region of -100% to -40%.

3.3. APD rate adaptation

Figure 3 shows the mean APD_{20}, APD_{50} and APD_{90} normalized to their appropriate values at 0.25 Hz. The curves representing experimental and model data overlap, indicating that the models reproduce APD rate dependence properties seen in experiments. To compare the absolute values of the APDs generated in experiments and through simulations, we need to ensure an even sampling of the biomarker space by the computational models. This can be achieved with the generation of two separate populations of models, one with short-to-medium APD values, and another one with high APDs, as briefly outlined in the previous section.

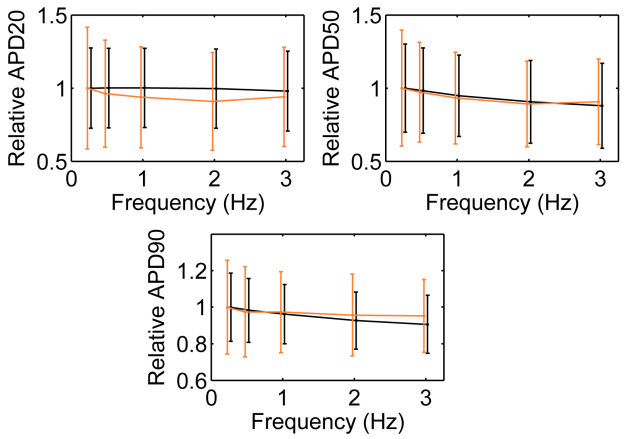

Figure 3. APD rate dependence plots. Mean values of APD_{20}, APD_{50} and APD_{90} are normalized to the values at 0.25 Hz. Legend: black – model predictions; orange – experimental data; error bars – standard deviation. The models capture experimental APD rate dependence.

4. Discussion and Conclusions

In this study, we constructed a population of single-cell models mimicking atrial myocytes extracted from a homogeneous patient group. Apart from the ionic conductances underpinning the AP, external factors such as the ionic concentrations and stimulus strength were found to play a critical role in producing the AP biomarker values consistent with experiments. For instance, APD90 and APA are significantly influenced by ionic conductances, while RMP and APD20 are critically dependent on ionic concentrations and stimulus strength. When these were taken into consideration, we were able to generate 604 models covering the experimentally allowed range of AP biomarker values. Furthermore, this final population of models captured the APD rate dependence properties observed in experimental data. Therefore, we demonstrated that both ionic conductances and external factors are critical in tailoring single-cell models of electrophysiology to a narrow patient group. This has implications in understanding the propensity of subgroups of the population to disease conditions.

We also explored the models of Courtemanche *et al.* [7] and Grandi *et al.* [8] describing human atrial electrophysiology in an attempt to build additional populations of models representative of the experimental data. However, none of these additional populations covered the biomarker space as well as the final 604 models based on the Maleckar *et al.* framework. There can be multiple reasons for this. Firstly, the baseline Grandi *et al.* and Courtemanche *et al.* models produce APs with a spike-and-dome morphology that are distinct from the triangular APs seen in experiments. This may reflect the large heterogeneity in AP morphology observed in different regions of the human atria, whereas all our experimental recordings where obtained in cells extracted form the right atrial appendage of patients in sinus rhythm. Additionally, the representation of biophysical processes, and in particular intracellular calcium handling, differs between the three models.

There were fewer models within the final population producing APD values at the higher end of experimental range due to downregulation in the transient outward potassium current. Future work will entail constructing two separate populations, one with short-to-medium APDs, and the other with long APDs. Investigations into the cause of different predictions between the three models of human atrial electrophysiology are also of interest.

Acknowledgements

AM is funded via an enhanced EPSRC stipend through the SysBio Doctoral Training Centre. ABO and BR are supported by BR Wellcome Trust Senior Research Fellowship in Basic Biomedical Sciences.

References

[1] Wilhelms M, *et al.* Benchmarking electrophysiological models of human atrial myocytes. Front Physiol 2013;3:487.

[2] Britton O, *et al.* Experimentally calibrated population of models predicts and explains intersubject variability in cardiac cellular electrophysiology. Proc Natl Acad Sci U S A 2013;110:E2098–105.

[3] Liu X, *et al.* Loss of myocardial nnos in atrial fibrillation (af) affects action potential duration: Implications for af-induced electrical remodelling. In Proc 37th IUPS. 2013; PCA055.

[4] Maleckar M, *et al.* K+ current changes account for the rate dependence of the action potential in the human atrial myocyte. Am J Physiol Heart Circ Physiol 2009;297:H1398–H1410.

[5] Pitt-Francis J, *et al.* Chaste: A test-driven approach to software development for biological modelling. Comput Phys Commun 2009;180:2452–2471.

[6] Cherry E, *et al.* Dynamics of human atrial cell models: Restitution, memory, and intracellular calcium dynamics in single cells. Prog Biophys Mol Bio 2008;98:24–37.

[7] Courtemanche M, *et al.* Ionic mechanisms underlying human atrial action potential properties: insights from a mathematical model. Am J Physiol Heart Circ Physiol 1998;275:H301–H321.

[8] Grandi E, *et al.* Human atrial action potential and Ca2+ model: sinus rhythm and chronic atrial fibrillation. Circ Res 2011;109:1055–1066.

Address for correspondence:

Anna Muszkiewicz
SysBio DTC, Rex Richards Building, South Parks Road, Oxford OX1 3QU, UK
anna.muszkiewicz@dtc.ox.ac.uk